

CrystEngComm

Accepted Manuscript



This is an *Accepted Manuscript*, which has been through the Royal Society of Chemistry peer review process and has been accepted for publication.

Accepted Manuscripts are published online shortly after acceptance, before technical editing, formatting and proof reading. Using this free service, authors can make their results available to the community, in citable form, before we publish the edited article. We will replace this *Accepted Manuscript* with the edited and formatted *Advance Article* as soon as it is available.

You can find more information about *Accepted Manuscripts* in the [Information for Authors](#).

Please note that technical editing may introduce minor changes to the text and/or graphics, which may alter content. The journal's standard [Terms & Conditions](#) and the [Ethical guidelines](#) still apply. In no event shall the Royal Society of Chemistry be held responsible for any errors or omissions in this *Accepted Manuscript* or any consequences arising from the use of any information it contains.

COMMUNICATION

Layer-by-Layer Assembly of L1₀-FePt Nanoparticles with Significant Perpendicular Magnetic Anisotropy

Cite this: DOI: 10.1039/x0xx00000x

Yunhe Dong,^a Fei Liu,^a Wenlong Yang,^a Jinghan Zhu,^a Jing Yu^a and Yanglong Hou^{a,*}

Received 00th January 2014,

Accepted 00th January 2014

DOI: 10.1039/x0xx00000x

www.rsc.org/

Abstract The ordered assembly of face-centered tetragonal (fct, L1₀) FePt nanoparticles (NPs) has been fabricated through a layer-by-layer assembly method under an external magnetic field. The assembled L1₀-FePt film with controlled magnetic alignment exhibits significant perpendicular magnetic anisotropy, which shows great potential for ultrahigh density data storage application.

The chemical synthesis and self-assembly of magnetic nanoparticles (NPs) including Fe,¹⁻² Co,³ FePt,⁴⁻⁶ CoPt⁷⁻⁸ and FeCo⁹ NPs have attracted extensive attention due to their great potential in magnetic nanodevice application. Particularly, developing magnetic NP arrays with controlled magnetic anisotropy is critical during constructing these assemblies, since the magnetic thin films with perpendicular anisotropy are easy to magnetize along a direction perpendicular to the film surface rather than randomly fluctuate over time. It is expected that the application of perpendicular magnetization will be able to build ultrahigh density vertical magnetic recording media and highly sensitive magnetotransport devices.¹⁰⁻¹² FePt alloy with a face-centered tetragonal (fct, L1₀) structure is considered as an ideal candidate due to the high magnetocrystalline anisotropy ($K = 7 \times 10^6 \text{ J/m}^3$), which is one of the largest value among the known hard magnetic materials.¹³ Such hard magnetic FePt NP films have been made by solvent evaporation of FePt NPs dispersion,^{4,14,15} but the subsequent thermal annealing conversion from face-centered cubic (fcc) to fct phase would result in degradation of the long-range ordering. In order to solve this problem and maintain the NPs well-dispersed, extra components are necessary. Dong¹⁶ and co-workers have reported the fabrication of L1₀-FePt nanocrystal superlattice membranes by co-assembly of FePt and MnO NPs at the liquid-air interface. Although the existence of MnO NPs protected FePt from sintering during the phase conversion, the L1₀-FePt film is limited to a fairly small range of area with controlled assembly structure. Furthermore, a common problem in these self-assembled L1₀-FePt NP films is that it is

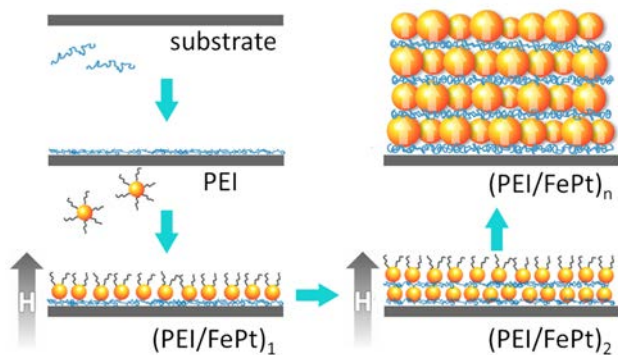
difficult to control the easy magnetization direction and to orient NPs along the easy axis direction. Therefore, the fabrication of L1₀-FePt NPs thin films with perpendicular c-axis orientations over an extended area is still a challenge to be met.

Layer-by-layer (LbL) self-assembly, regarded as a versatile bottom-up nanofabrication technique, has been successfully utilized to prepare various homogeneous ultrathin films over large areas for electrical, magnetic, catalytic and optical applications.¹⁷⁻²³ The LbL assembly technique developed by Decher and co-workers^{24,25} can be applied to a wide range of materials on a large scale to obtain highly controlled multilayered micro-architectures. LbL-assembled films are mainly conducted through electrostatic interaction,^{19-21,23-26} hydrogen bonding,^{17,22} or covalent bonding²⁷ in the context of an aqueous media. An assembly of ferromagnetic FePt NPs exhibiting perpendicular magnetic anisotropy has been obtained by depositing cationic polyelectrolyte azobenzene polymer and L1₀-FePt NPs dispersed in water under a strong magnetic field.²⁸ More recently, a general approach based on an in situ ligand exchange between the hydrophobic NPs stabilizers and the polymer amine groups is introduced to prepare functional nanocomposite multilayers,²⁹ which offers a facile and effective method to generate L1₀-FePt LbL-assembled films in an organic medium. However, it is rarely reported about assembled L1₀-FePt NPs films exhibiting larger magnetic anisotropy, which is highly expected for potential application of high density data storage. Thus the assembly of fct-FePt NPs with higher coercivity shows a compelling need.

In this paper, monodisperse L1₀-FePt NPs with a coercivity of 31.7 kOe have been successfully synthesized and used as building blocks for self-assembly. A LbL-assembly method by consecutively alternating adsorption of the polyethylenimine (PEI) and L1₀-FePt NPs is applied to prepare the ferromagnetic NP assembly. In order to enhance its performance for perpendicular magnetic recording media, the (PEI/L1₀-FePt)_n multilayers were prepared by applying an external magnetic field during the LbL self-assembly. This directly-developed (PEI/L1₀-FePt)_n assemblies without thermal annealing process are expected to exhibit significant perpendicular magnetic

anisotropy with high coercive force and high remanence at room temperature.

The fabrication of macroscopic multilayer films of PEI and $L1_0$ -FePt NPs is depicted in detail as shown in Scheme 1. A well-cleaned substrate is immersed into ethanol solution of PEI for 5 min, followed by rinsing with ethanol and drying in a gentle nitrogen stream. Subsequently, the PEI-coated substrate is dipped into toluene dispersion of the $L1_0$ -FePt NPs for 10 min. After rinsed in toluene, the substrate was then placed horizontally on a strong magnet with a magnetic field normal to the film surface immediately and dried with a gentle N_2 flow. By repeating this procedure in cycles, the assembly of magnetic NPs with oriented magnetic moments can be obtained. This magnetic-field-assisted LbL self-assembly is based on an in situ ligand exchange between the hydrophobic NPs ($L1_0$ -FePt) stabilizers and the polymer amine groups (PEI) in an organic medium, which has been proved effective in building multilayer films.²⁹ When $L1_0$ -FePt NPs were deposited onto the PEI-coated substrates, oleic acid/oleylamine bound to the bottom surface of $L1_0$ -FePt NPs can be easily replaced by the amine groups in PEI. Along with the next absorption of PEI layer, ligand exchange is completed between amine-functionalized PEI and the remaining oleic acid/oleylamine around the top surface of fct-FePt NPs. A strong PEI-protected NPs assembly is resulted from consecutive deposition of PEI and $L1_0$ -FePt NPs onto the substrates via LbL-assembly method.



Scheme 1 Schematic illustration for $(PEI/L1_0-FePt)_n$ multilayers via magnetic-field-assisted LbL self-assembly method.

The $L1_0$ -FePt NPs used as building blocks were prepared by modifying a previously reported procedure by our group.³⁰ Briefly, the fcc-FePt NPs are synthesized by simultaneous reduction of platinum acetylacetonate ($Pt(acac)_2$) and iron pentacarbonyl ($Fe(CO)_5$) and coated with a layer of MgO by decomposition of magnesium(II) acetylacetonate hydrate ($Mg(acac)_2 \cdot 2H_2O$) in the presence of oleic acid and oleylamine in benzyl ether. After the thermal annealing of fcc-FePt/MgO NPs at $700^\circ C$ in Ar containing 5% H_2 , $L1_0$ -FePt/MgO NPs are obtained and treated with nitric acid to remove MgO shell. These $L1_0$ -FePt NPs are further treated in toluene containing oleic acid, oleylamine and 1-hexadecanethiol at $100^\circ C$, and can be dispersed in toluene or hexane. The detailed synthetic process and the intermediate product are shown in supporting information and Figure S1. As revealed in the TEM image of Figure 1a, the $L1_0$ -FePt NPs are successfully produced with an average particle size of around 8 nm and good dispersibility in toluene, facilitating assembling the NPs with the magnetic easy axes preferably aligned to the external magnetic field. The ratio of Fe and Pt in the $L1_0$ -FePt NPs was 50 : 50 according to inductively coupled plasma atomic emission spectroscopy (ICP-AES). Figure 1b displays a high-resolution TEM (HRTEM) image of a single $L1_0$ -FePt particle with high crystallinity. The $L1_0$ -FePt NP has a lattice fringe

of 0.27 nm, corresponding to the lattice spacing of the (110) planes in the $L1_0$ -FePt. Figure 1c is a typical selected area electron diffraction (SAED) pattern of the $L1_0$ -FePt NPs shown in Figure 1a. The (001), (110), (111), (200) and (002) rings can be clearly seen, which are characteristics of the $L1_0$ -structure. The crystal structure of the $L1_0$ -FePt NPs was further characterized by X-ray diffraction (XRD) shown in Figure 1d. The XRD pattern fits well to the standard pattern of $L1_0$ -FePt (JCPDS ICDD card 43-1359). Two characteristic diffraction peaks of (001) and (200) planes at the diffraction angle of 47° and 49° occur in the patterns respectively, indicating the formation of $L1_0$ structure.

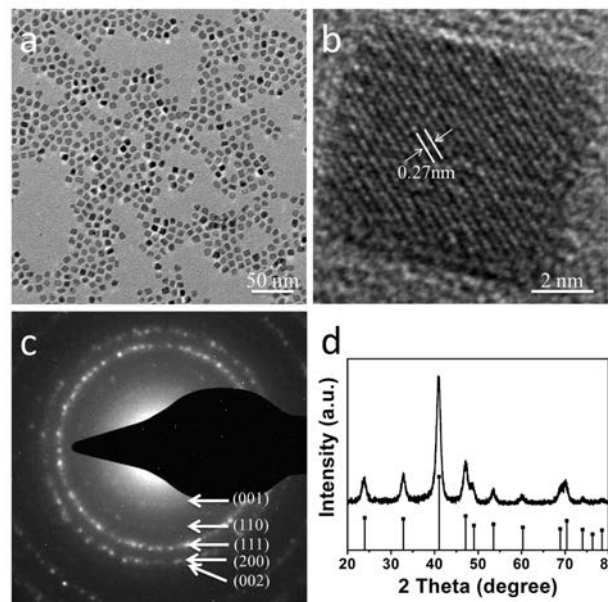


Figure 1 (a) TEM image of the fct-FePt NPs, (b) HRTEM image of a single nanoparticle, (c) SAED pattern and (d) XRD pattern of the $L1_0$ -FePt NPs.

The ligand-exchange strategy of this LbL-assembly method was examined by Fourier transform infrared (FTIR) spectroscopy in attenuated total reflection (ATR) mode (Figure 2a). The absorption peaks of PEI occurred at $3300-3500\text{ cm}^{-1}$ originating from the N-H stretching vibration and $1650-1515\text{ cm}^{-1}$ resulting from the N-H bending vibration, respectively. The ATR-FTIR spectra of the $L1_0$ -FePt NPs displayed absorption peaks assigned to the carbonyl ($C=O$) stretching vibration at 1710 cm^{-1} . As the PEI layer was adsorbed onto the $L1_0$ -FePt NPs layer, the absorption peak intensity corresponding to the $C=O$ stretching at 1710 cm^{-1} disappeared in the spectra of PEI/ $L1_0$ -FePt film. These results evidently indicate that the oleic acid/oleylamine ligands bound to $L1_0$ -FePt NPs were exchanged with PEI chains. In this LbL assembly process, an in situ ligand-exchange occurs and PEI/fct-FePt assembly is formed.

A key feature of the fabrication of $(PEI/L1_0-FePt)_n$ multilayered architecture is control of individual layer formation. The TEM bright field image of a single PEI/ $L1_0$ -FePt multilayer assembled on TEM grids is shown in Figure 2b (Figure S2) with an enlarged TEM image of an area in the inset. The adsorbed $L1_0$ -FePt NPs exhibit a dense packing density per layer on a large scale with the layer packing density of approximately 60%, which is in accordance with the value reported previously.²⁹ It is worth noting that the colloidal $L1_0$ -FePt single layer formed on PEI exhibits greater surface coverage than that obtained from aqueous solution. The difference is due to electrostatic repulsions of the same charged NPs in water.

The growth process of $(\text{PEI}/\text{L1}_0\text{-FePt})_n$ LbL-assembled film was monitored by UV-vis spectroscopy. The quartz glasses are used as substrates for alternately deposition of PEI and $\text{L1}_0\text{-FePt}$ NPs. UV-vis spectra (Figure 2c) show the linear increase of the monolithic absorbance after each deposition process, and the inset diagram demonstrates that the absorption intensity at 400 nm exhibits a monotonic increase along with increasing bilayer number (n). This linearity confirms a stepwise and uniform deposition procedure in each cycle, which can be ascribed to in situ ligand exchange from oleic acid/oleylamine ligands to PEI.

When such films are prepared on silicon wafers, an approximately linear increase of the film thickness with various number of layers is observed by the cross-sectional scanning electron microscopy (SEM) images of the films (Figure 2d). The average growth increment per bilayer cycle estimated from SEM images is 10 nm, which is close to the thickness of the single layer of $\text{L1}_0\text{-FePt}$ NPs (~ 8 nm) and PEI (~ 2 nm).

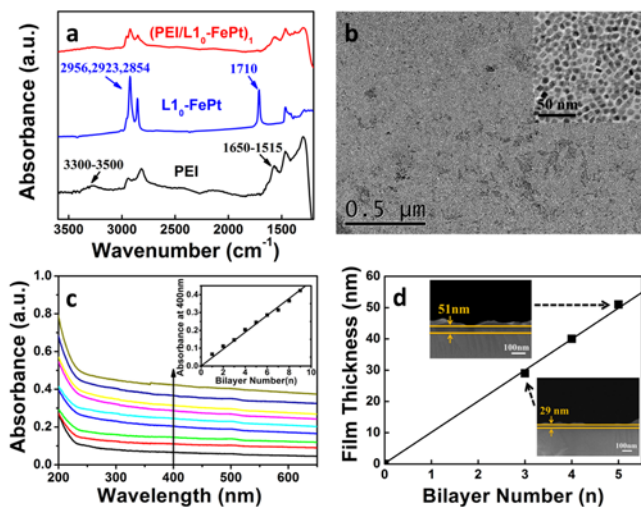


Figure 2 (a) ATR-FTIR spectra of PEI, $\text{L1}_0\text{-FePt}$, and $(\text{PEI}/\text{L1}_0\text{-FePt})_n$ films, (b) An overview TEM image and high magnification TEM image of a 8 nm sized $\text{L1}_0\text{-FePt}$ NPs single layer assembled on PEI-coated TEM grids, (c) UV-vis spectra of $(\text{PEI}/\text{L1}_0\text{-FePt})_n$ multilayers on quartz glass as a function of bilayer number (n). The insets is the plot of absorbance at 400nm for $(\text{PEI}/\text{L1}_0\text{-FePt})_n$ multilayers versus the bilayer number, (d) Film thickness of $(\text{PEI}/\text{L1}_0\text{-FePt})_n$ multilayers on silicon substrates as a function of bilayer number. The inset shows the side-view SEM images of the films.

Room-temperature hysteresis loops of $(\text{PEI}/\text{L1}_0\text{-FePt})_5$ films via a LbL self-assembly method with and without an external magnetic field are shown in Figure 3. The $\text{L1}_0\text{-FePt}$ powders are ferromagnetic at room temperature with a large coercivity of 31.7 kOe and a saturation magnetization (M_s) of 36 emu g^{-1} (Figure S3). When the $\text{L1}_0\text{-FePt}$ NPs are assembled on silicon substrate without the external magnetic field (Figure 3a), no apparent difference is observed in the out-of-plane and in-plane loops, where the magnetic fields are perpendicular and parallel to the film surface respectively. From Figure 3b, it can be seen that the $(\text{PEI}/\text{L1}_0\text{-FePt})_n$ film assembled under an external magnetic field exhibits an extremely high coercivity of 34.9 kOe and a high remanence ratio (M_r/M_s) of 0.80 in the out-of-plane direction, which are considerably higher than those in Figure 3a. As a comparison, the in-plane loop shows the coercivity of 13.1 kOe and the remanence ratio of 0.34, indicating that the magnetic easy axes are aligned preferably perpendicular to the film surface. The kink where the magnetic field is around zero is

ascribed to the magnetostatic interaction between the hard magnetic particles.^{31,32} These ferromagnetic $\text{L1}_0\text{-FePt}$ NP assembly exhibiting large perpendicular magnetic anisotropy could be regarded as a strong candidate for ultrahigh-density magnetic recording media with the capability of achieving densities of terabits/in².

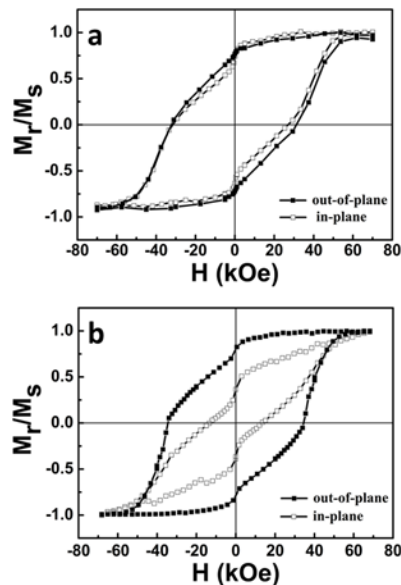


Figure 3 Room-temperature hysteresis loops of $(\text{PEI}/\text{L1}_0\text{-FePt})_n$ films assembled without (a) and under (b) an external magnetic field in the out-of-plane and in-plane direction, where $n=5$.

In conclusion, we report the synthesis of monodisperse $\text{L1}_0\text{-FePt}$ NPs readily dispersed in toluene and the preparation of an assembly of $\text{L1}_0\text{-FePt}$ NPs via a versatile LbL self-assembly method by alternating deposition of PEI and $\text{L1}_0\text{-FePt}$ NPs under an external magnetic field. ATR-FTIR spectra indicate the occurrence of ligand-exchange between PEI chains and the ligands bound to $\text{L1}_0\text{-FePt}$ NPs. A uniform and high surface coverage assembly film has been fabricated which can be demonstrated by TEM images, UV-vis spectra, and side-view SEM images of the multilayer film. As a result, significant perpendicular magnetic anisotropy at room temperature has been observed in $(\text{PEI}/\text{L1}_0\text{-FePt})_n$ multilayers film. These ferromagnetic NPs show the preferred magnetic alignment with a coercivity of 34.9 kOe. It is expected that the strategy described in this work could also be extended to the fabrication of the exchange-coupled hard/soft magnetic NPs composite films.

Acknowledgments. This work was supported in part by the Natural Science Foundation of Beijing (2122022), the National Basic Research Program of China (2010CB934601), the NSFC (51125001, 51172005), and the Doctoral Program (20120001110078).

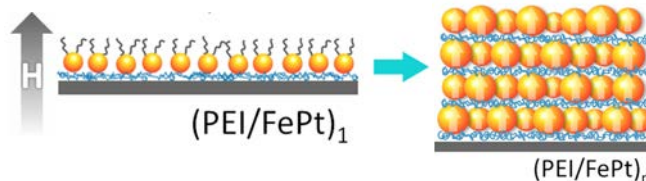
† **Electronic Supplementary Information (ESI) available:** Experimental details, Film preparation, Characterization Methods, TEM images of the intermediate product in the synthesis process and a single layer, Room-temperature hysteresis loops of $\text{L1}_0\text{-FePt}$ powders. See DOI: 10.1039/b000000x/

Notes and references

Department of Materials Science and Engineering, College of Engineering, Peking University, Beijing, 100871, China. E-mail: hou@pku.edu.cn; Fax: 86-10-62753115

- 1 S. Zhang, G. Jiang, G. Filsinger, L. Wu, H. Zhu, J. Lee, Z. Wu and S. Sun, *Nanoscale*, 2014, **6**, 4852.
- 2 S.-J. Park, S. Kim, S. Lee, Z. G. Khim, K. Char and T. Hyeon, *J. Am. Chem. Soc.*, 2000, **122**, 8581.
- 3 S. Sun and C. B. Murray, *J. Appl. Phys.*, 1999, **85**, 4325.
- 4 S. Sun, C. Murray, D. Weller, L. Folks and A. Moser, *Science*, 2000, **287**, 1989.
- 5 M. Chen, J. Kim, J. P. Liu, H. Fan and S. Sun, *J. Am. Chem. Soc.*, 2006, **128**, 7132.
- 6 J. Wu, J. Zhu, M. Zhou, Y. Hou and S. Gao, *CrystEngComm*, 2012, **14**, 7572.
- 7 J.-I. Park and J. Cheon, *J. Am. Chem. Soc.*, 2001, **123**, 5743.
- 8 E. V. Shevchenko, D. V. Talapin, A. L. Rogach, A. Kornowski, M. Haase and H. Weller, *J. Am. Chem. Soc.*, 2002, **124**, 11480.
- 9 C. Desvaux, C. Amiens, P. Fejes, P. Renaud, M. Respaud, P. Lecante, E. Snoeck and B. Chaudret, *Nat. Mater.*, 2005, **4**, 750.
- 10 B. Balasubramanian, B. Das, R. Skomski, W. Y. Zhang and D. J. Sellmyer, *Adv. Mater.*, 2013, **25**, 6090.
- 11 P. Carcia, A. Meinhardt and A. Suna, *Appl. Phys. Lett.*, 1985, **47**, 178.
- 12 C. Wang, Y. Hou, J. Kim and S. Sun, *Angew. Chem. Int. Ed.*, 2007, **46**, 6333.
- 13 D. Weller, A. Moser, L. Folks, M. E. Best, W. Lee, M. F. Toney, M. Schwickert, J.-U. Thiele and M. F. Doerner, *IEEE Trans. Magn.*, 2000, **36**, 10.
- 14 L. C. Varanda and M. Jafelicci, *J. Am. Chem. Soc.*, 2006, **128**, 11062.
- 15 S. Sun, E. E. Fullerton, D. Weller and C. Murray, *IEEE Trans. Magn.*, 2001, **37**, 1239.
- 16 A. Dong, J. Chen, X. Ye, J. M. Kikkawa and C. B. Murray, *J. Am. Chem. Soc.*, 2011, **133**, 13296.
- 17 S. W. Lee, J. Kim, S. Chen, P. T. Hammond and Y. Shao-Horn, *ACS Nano*, 2010, **4**, 3889.
- 18 S. Sun, S. Anders, H. F. Hamann, J.-U. Thiele, J. Baglin, T. Thomson, E. E. Fullerton, C. Murray and B. D. Terris, *J. Am. Chem. Soc.*, 2002, **124**, 2884.
- 19 F.-X. Xiao, J. Miao and B. Liu, *J. Am. Chem. Soc.*, 2014, **136**, 1559.
- 20 R. Liang, R. Tian, W. Shi, Z. Liu, D. Yan, M. Wei, D. G. Evans and X. Duan, *Chem. Commun.*, 2013, **49**, 969.
- 21 X. Li, M.-Q. Zha, S.-Y. Gao, P. J. Low, Y.-Z. Wu, N. Gan and R. Cao, *CrystEngComm*, 2011, **13**, 920.
- 22 P. Podsiadlo, A. K. Kaushik, E. M. Arruda, A. M. Waas, B. S. Shim, J. Xu, H. Nandivada, B. G. Pumplun, J. Lahann, A. Ramamoorthy and N. A. Kotov, *Science*, 2007, **318**, 80.
- 23 W. K. Bae, J. Kwak, J. Lim, D. Lee, M. K. Nam, K. Char, C. Lee and S. Lee, *Nano Lett.*, 2010, **10**, 2368.
- 24 G. Decher, J. D. Hong and J. Schmitt, *Thin Solid Films*, 1992, **210–211, Part 2**, 831.
- 25 G. Decher, *Science*, 1997, **277**, 1232.
- 26 S. S. Qureshi, Z. Zheng, M. I. Sarwar, O. Félix and G. Decher, *ACS Nano*, 2013, **7**, 9336.
- 27 G. K. Such, J. F. Quinn, A. Quinn, E. Tjijto and F. Caruso, *J. Am. Chem. Soc.*, 2006, **128**, 9318.
- 28 M. Suda and Y. Einaga, *Angew. Chem. Int. Ed.*, 2009, **48**, 1754.
- 29 Y. Ko, H. Baek, Y. Kim, M. Yoon and J. Cho, *ACS Nano*, 2012, **7**, 143.
- 30 F. Liu, J. Zhu, W. Yang, Y. Dong, Y. Hou, C. Zhang, H. Yin and S. Sun, *Angew. Chem. Int. Ed.*, 2014, **53**, 2176.
- 31 V. Novosad, K. Y. Guslienko, H. Shima, Y. Otani, S. Kim, K. Fukamichi, N. Kikuchi, O. Kitakami and Y. Shimada, *Phys. Rev. B*, 2002, **65**, 060402.1.
- 32 V. Novosad, M. Grimsditch, J. Darrouzet, J. Pearson, S. Bader, V. Metlushko, K. Guslienko, Y. Otani, H. Shima and K. Fukamichi, *Appl. Phys. Lett.*, 2003, **82**, 3716.

A table of contents entry.



Text:

The $L1_0$ -FePt film has been fabricated via layer-by-layer assembly under an external magnetic field, which exhibits significant perpendicular magnetic anisotropy.